



Global contour shapes are coded differently from their local components

Jason Bell*, Fredrick A.A. Kingdom

McGill Vision Research, Department of Ophthalmology, McGill University, 687 Pine Avenue West, H4-14, Montreal, Quebec, Canada H3A 1A1

ARTICLE INFO

Article history:

Received 16 December 2008

Received in revised form 25 March 2009

Keywords:

Adaptation

Global

Curvature

Contour

Radial frequency

ABSTRACT

Previous research has shown that the mechanisms that process curved contours are selective for low-level attributes such as luminance contrast polarity and luminance spatial-frequency, while those that process curvature-defined global shapes are not. While these findings are consistent with the view that higher stages of object processing are relatively agnostic to low-level attributes, methodological differences (appearance-based tasks in the former versus performance-based tasks in the latter) might instead be the reason. In this study, we demonstrate a radial frequency pattern analog of the shape-amplitude after-effect, or SAAE, termed the radial frequency amplitude after-effect, or RFAAE. We use the RFAAE to investigate whether global contour shapes are represented differently from their local components. Results show that the RFAAE, like the SAAE, is bidirectional (perceived amplitude can be shifted by adaptation in either direction), showing that RF-shape mechanisms are selective for amplitude. However, unlike the SAAE, the RFAAE is not selective for luminance contrast polarity or for luminance spatial-frequency. These findings using an appearance-based approach reinforce the conclusions from previous performance-based studies that global contour shapes are coded differently from their local components.

Crown Copyright © 2009 Published by Elsevier Ltd. All rights reserved.

1. Introduction

An important function of vision is to detect and recognize objects within the natural environment, and the perception of an object's shape is critical to this end (Attneave, 1954; Biederman, 1987; Loffler, Yourganov, Wilkinson, & Wilson, 2005). The aim of the current study is to determine whether the representation of 'global' shapes is qualitatively different from the representation of the local components that make up those shapes. It is widely believed that shape processing proceeds through a hierarchy of stages of increasing complexity, beginning with the processing of local orientation, then of local curvature, and finally of global shape (Badcock & Clifford, 2006; Lennie, 1998; Lerner, Hendler, Ben-Bashat, Harel, & Malach, 2001; Poirier & Wilson, 2006; Wilson & Wilkinson, 1998; Wilson, Wilkinson, & Asaad, 1997). This hierarchy also involves feedback from higher to lower cortical regions (Lamme, Super, & Spekreijse, 1998; Murray, Kersten, Olshausen, Schrater, & Woods, 2002; Roach, Webb, & McGraw, 2008).

Various lines of evidence point to the idea that as one proceeds through these stages, the visual system increasingly discards information about low-level attributes such as edge phase (or polarity), scale, position etc. with the result that the highest stages of shape processing are agnostic to these attributes (Betts, Rainville, & Wilson, 2008; Grill-Spector, Kushnir, Edelman, Itzchak, & Malach, 1998; Murray & He, 2006; Okusa, Kakigi, & Osaka, 2000). This ac-

cords with the belief that higher visual stages are concerned with recognizing that an object is one and the same not only when defined by different low-level attributes such as phase, scale, position etc., but also when viewed from different angles (Bell, Dickinson, & Badcock, 2008; Burke, Taubert, & Higman, 2007; Grill-Spector et al., 1999; Jeffery, Rhodes, & Busey, 2006).

The psychophysical evidence that lower stages of shape processing are sensitive to, whereas higher-level stages are agnostic to low-level attributes, is, however, piece-meal. Studies of contour curvature after-effects have revealed that curvature mechanisms are selective for low-level attributes such as luminance polarity, luminance spatial-frequency and luminance contrast (Gheorghiu & Kingdom, 2006, 2007b, 2008). Studies of global-shape threshold-discrimination on the other hand have reported non-selectivity to these attributes as well as to the size of the shapes (Achtman, Hess, & Wang, 2000; Anderson, Habak, Wilkinson, & Wilson, 2007; Bell & Badcock, 2008; Bell, Badcock, Wilson, & Wilkinson, 2007a; Bell et al., 2008; Wilkinson, Wilson, & Habak, 1998). The curvature after-effect and global-shape studies however employed different methodologies: appearance-based methods for the curvature after-effects; performance-based methods for the global-shape discrimination thresholds. There is a compelling argument that appearance-based and performance-based measures of shape perception tap different visual processes (Gheorghiu & Kingdom, 2008; Loffler, 2008). Specifically, contour-shape discrimination-threshold tasks are likely mediated by relatively simple neural machinery, whereas the neural machinery involved in appearance-based shape tasks is likely more complex because the dimen-

* Corresponding author.

E-mail address: jason.bell@mail.mcgill.ca (J. Bell).

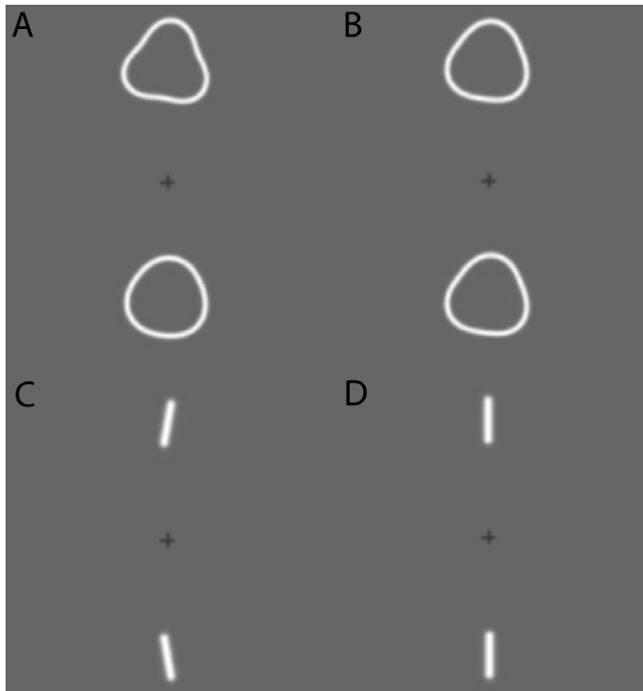


Fig. 1. Examples of the stimuli used in this study. (A and B) To experience the radial frequency amplitude after-effect (RFAAE) simply stare at the fixation cross corresponding to location A for at least 30 s. Next, shift your gaze to the fixation cross between the RF test pair at location B. Although the two test patterns are physically equal in amplitude, the upper pattern should appear lower in amplitude than the lower pattern. (C and D) To experience the tilt after-effect (TAE), stare at the fixation cross between the two line elements at C for at least 30 s. Next, shift your gaze to the fixation cross at D. Although the two lines are physically vertical, the upper may appear rotated anti-clockwise from vertical while the lower may appear rotated clockwise from vertical.

sion of interest (curvature and global shape) has to be explicitly represented (Gheorghiu & Kingdom, 2008). Thus the differences in the measured selectivity to low-level attributes in the aforementioned curvature and global-shape studies may be due to their different neural requirements rather than because they are mediated by different stages of shape processing. The aim of this communication is to establish whether or not this is the case.

A type of global shape that is popular among vision scientists because it lends itself to parametric investigation is the radial frequency, or RF pattern, an example of which is illustrated in Fig. 1. The RF pattern is a perturbed circle that can be characterized by its average radius, amplitude and radial frequency (Wilkinson et al., 1998). The detection of RF patterns (that is the discriminability of RF patterns from circles) appears to involve integration of local form cues such as local orientation and/or curvature (Bell & Badcock, 2008; Bell et al., 2008; Hess, Wang, & Dakin, 1999; Jeffrey, Wang, & Birch, 2002; Loffler, Wilson, & Wilkinson, 2003). This makes RF patterns appropriate stimuli for investigating whether curvature information is represented differently when integrated into a global shape compared to when presented alone.

The current study investigates whether the representation of an RF pattern is as selective to scale and luminance polarity as are the curves that make up the pattern. The experiments all use an RF analog of the shape-amplitude after-effect (SAAE) employed by Gheorghiu and Kingdom (2006, 2007a, 2007b, 2008) for measuring curvature after-effects. Note that with RF patterns one cannot measure an analog of the shape-frequency after-effect (SFAE) because radial frequency can only be specified in integer numbers of cycles.

2. Methods

2.1. Participants

Four experienced psychophysical observers participated in the current study. Three were naïve as to the experimental aims, while observer (JB) was an author. All had normal or corrected-to-normal visual acuity. Participation was voluntary and unpaid.

2.2. Apparatus and stimuli

Stimuli were created using Matlab version 7.6, and loaded into the frame-store of a Cambridge Research Systems (CRS) Visage video-graphics system. Stimuli were presented on a Sony Trinitron G400 monitor with a screen resolution of 768×1024 pixels and a refresh rate of 100 Hz. The luminance of the monitor was calibrated using an Optical OP200-E (Head Model # 265). The mean luminance of the monitor was 50.4 cd/m^2 .

The adaptation and test stimuli consisted of pairs of radial frequency (RF) contours, or in the case of Experiment 2, pairs of line elements (see Fig. 1). RF contours were created by modulating the radius of a circle using a sinusoidal function

$$r(\theta) = r_{\text{mean}}(1 + A \sin(\omega\theta + \varphi)) \quad (1)$$

Here r (radius) and θ (angle) represent the polar coordinates of the contour and r_{mean} is the average radius of the contour. A is the amplitude of pattern deformation (between 0 and 1), ω determines the RF number and φ the angular phase (orientation) of the shape. Fig. 1A and B shows example RF3 contours for adaptor (A) and test (B) pairs. In Experiments 1, 3, 4 and 5 the cross-sectional luminance profile of the RF contours was a Gaussian envelope with sigma 0.085° . In Experiment 2, the RF contours and the line elements had a cross-sectional luminance profile consistent with the fourth derivative of a Gaussian (D4). A D4 was chosen because it gives the stimulus a narrow and specifiable luminance spatial-frequency bandwidth (Wilkinson et al., 1998), enabling us to test the effect of changes in luminance spatial-frequency on the size of the shape after-effects. In all conditions, individual adaptation and test stimuli were presented 3° above or below a central grey fixation cross (the distance given is the center of the pattern to the center of the fixation cross). Unless otherwise stated, the spatial location corresponding to the center of each pattern was spatially jittered on each trial up to 0.25° in any direction.

2.3. Procedure

A staircase procedure was employed to measure both the shape-amplitude after-effect in RF patterns, termed here the radial frequency amplitude after-effect, or RFAAE, and the tilt after-effect with lines. The procedure was the same as that used by Gheorghiu and Kingdom (2006, 2007a, 2007b, 2008) for measuring the SFAE and SAAE.

2.3.1. RF conditions – dual adaptor method

The adaptation period lasted 1 min, during which either the spatial location, or the angular phase of each RF adapting pattern was jittered every 500 ms. Unless otherwise stated, the amplitudes (A in Eq. (1)) of the adapting patterns were 0.05 and 0.15, giving a geometric mean of 0.086 (see Fig. 1A and B). Each cycle of the test period began with a 400 ms blank screen, followed by the test pair for 500 ms (signaled by a tone), then a blank screen of 100 ms and finally 2.5 s top-up adaptation. The test pair were presented simultaneously 3° above and 3° below the fixation cross and the observer was instructed to select whether the upper or lower test pattern appeared to be the more deformed from circularity (or the higher in amplitude [A in Eq. (1)]). The amplitude ratio of the test patterns on the first test trial was set to a random number be-

tween 0.5 and 1.5 (upper divided by lower) but with geometric mean amplitude fixed at 0.086 (Fig. 1B). Following each response (a key press) the computer adjusted the ratio of amplitudes in a direction opposite to that of the response, i.e. towards the point of subjective equality (PSE). For the first six trials, the ratio was adjusted by a factor of 1.12, and thereafter by a factor of 1.06. Each run was terminated after 25 trials and the PSE was calculated as the geometric mean ratio of test pattern amplitudes over the last 20 trials, which on average contained 6–10 reversals. Typically, six PSEs were measured for each condition. In half of the sessions, the high amplitude adapting pattern was in the upper visual field whereas in the other half of the sessions the lower amplitude adapting pattern was in the upper visual field. In addition, we measured the PSE in sessions containing no adaptation stimuli; these served as baselines with which to compare the size of the RFAAE with adaptation. The size of the after-effect calculated for each session was given by the log ratio of test amplitudes (corresponding to the lower and higher adapting amplitudes) at the PSE minus the same PSE value without adaptation. The mean and SE of these values across sessions are the points shown in the graphs.

2.3.2. RF conditions – single adaptor method

In order to determine if the RFAAE was unidirectional (all adaptors caused tests to look higher, or lower in amplitude) or bi-directional (low amplitude adaptors caused higher amplitude test to look higher, whereas higher amplitude adaptors caused lower amplitude test to look lower), we used a single adaptor method (Experiments 4 and 5). In each session a single adapting pattern was presented, either in the upper or lower field (equal numbers of both and in random order). The test pattern was presented in the same retinal location as the adapting pattern, while a comparison pattern was shown in the opposite hemi-field. The test was fixed in amplitude at 0.1 while the comparison amplitude was adjusted using the same staircase procedure. All other aspects of procedure were the same as for the dual adaptor method.

2.3.3. Line element conditions – dual adaptor method

The tilt-after-effect was measured using line stimuli as shown in Fig. 1. The lines were presented 3° above or below fixation. The adapting lines were oriented 10° clockwise and 10° anti-clockwise from vertical (Fig. 1C) and the observer was instructed to indicate which of two line elements appeared clockwise from vertical. Following the observer's response, the staircase procedure adjusted the orientation of the upper and lower test lines towards the PSE (Fig. 1D). For the first six trials, 1° was added to or subtracted from the orientation of each test line; thereafter 0.5° steps were used. The relative orientations of the upper and lower test lines were symmetrical about vertical, with the same angular change added to one being subtracted from the other. Rather than recording the ratio of the two, in these conditions the angular difference between elements was measured. If negative, the number was multiplied by –1 so that the angular difference was always positive. The angular difference over the last 20 trials was used to calculate the mean difference and std. error at the PSE in each condition. We also ran trials involving no adaptation, in order to measure the average angular difference between elements in these cases (baseline). The data shown plots the average angular difference between elements following adaptation, minus the baseline measurement.

3. Experiments

3.1. Experiment 1: the radial frequency amplitude after-effect (RFAAE)

In order to compare the selectivity of global-shape- and curvature-sensitive mechanisms to low-level attributes such as lumi-

nance polarity and scale, it seems sensible to use a similar methodology. Selectivity to low-level attributes in curvature processing has been revealed previously through two shape after-effects, the shape-frequency and shape-amplitude after-effects, or SFAE and SAAE (Gheorghiu & Kingdom, 2006, 2007b). As we stated in the introduction, one cannot measure a SFAE analog for RF patterns because RF patterns can only be defined by integer numbers of cycles. However a SAAE analog is entirely possible because RF amplitude is a continuous variable. Experiment 1 establishes two things: (a) that there exists a 'radial frequency amplitude after-effect', or RFAAE and (b) its degree of selectivity to luminance contrast polarity.

Fig. 2 shows the results for four observers using the dual adaptor method. Subjects adapted to two RF contours with different amplitudes in the upper and lower visual fields, and adjusted two test contours until they appeared equal in perceived amplitude. The adapting and test patterns were fixed in relative angular phase but independently jittered in spatial location on each trial (for the adapting patterns every 500 ms). It is clear that for each observer and for all polarity combinations, adaptation causes a significant shift in the perceived amplitude of the test RF contours. A repeated measures two-way ANOVA between the size of after-effect with and without adaptation was highly significant ($F_{(2,12)} = 205.5, p < .0001$). There were no significant differences between the size of the after-effect for Bright and Dark RF test patterns ($F_{(1,12)} = 0.2, p = .67$). The size of the after-effect for the crossed polarity conditions was about 80% of that of the same polarity conditions, and the difference was just significant ([Bonferroni post-hoc] Bright test: *same polarity versus opposite*: $p < .05$; Dark test: *same polarity versus opposite*: $p < .05$).

The size of the RFAAE reported here is on average larger than the analogous after-effect with sinusoidal-shaped contours – the SAAE (Gheorghiu & Kingdom, 2007b, 2008). However in the studies of the SAAE, the shape-phases of the adapting sine-wave contours were randomized every 500 ms. Therefore we ran a second experiment in which we measured the RFAAE when the angular phase of the adapting and test patterns was randomized on each trial (every 500 ms for the adapting pattern). The spatial locations of the adapting and test patterns were fixed. All other parameters were the same as for the previous experiment. The results are shown in Fig. 3. Since there were no differences between the Bright and Dark test pattern results, we report the results for a Bright test pattern following adaptation to patterns of the same (B/B) or opposite (D/B) contrast polarity. As in the previous experiment, adaptation had a significant effect on the perceived amplitude of the test RF patterns ($F_{(2,6)} = 27.21, p < .001$). However, the RFAAE is smaller than that for the fixed-phase patterns, and is similar in magnitude to the SAAE reported by Gheorghiu and Kingdom (2007b, 2008). More interestingly, there is now only a moderate transfer (60%) between opposite polarity adaptors and tests, and the difference between same-polarity and opposite-polarity conditions is significant ([Bonferroni post-hoc] $p < .05$).

The results of both experiments demonstrate a radial frequency amplitude after-effect, or RFAAE, that is greater for fixed compared to random-phase patterns. The larger after-effect in the fixed-phase patterns might be due to the combined contributions of local orientation adaptation, i.e. the tilt after-effect and global-shape adaptation. Since the tilt after-effect is reportedly not tuned for contrast polarity (Magnussen & Kurtenbach, 1979), it is possible that the tilt after-effect is responsible for the relatively large degree of transfer across contrast polarity in the fixed-phase condition, rather than the global-shape mechanism being agnostic to changes in contrast polarity. Experiment 2 was designed to investigate the relative contribution of local orientation adaptation to the RFAAE in order to determine whether the polarity results of Experiment 1 can be explained by local TAEs.

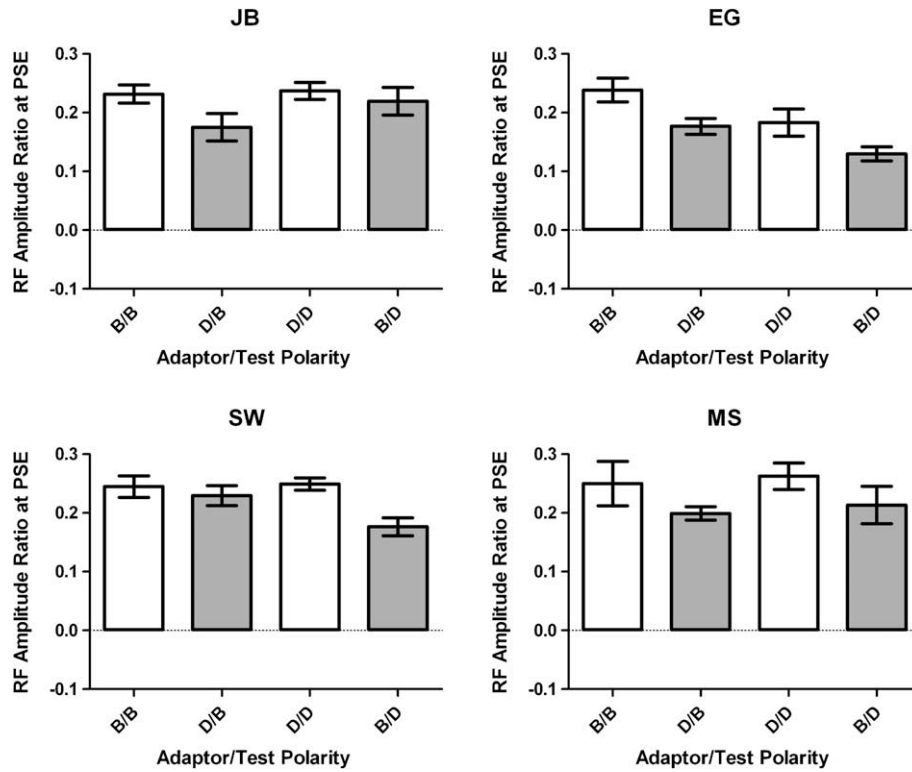


Fig. 2. RFAAEs for four observers with adaptor-test combinations which are either the same (Clear bars) or opposite (Grey bars) contrast polarity. The different types of contour are: ‘B’, Bright; ‘D’, Dark. D/B indicates a Dark adaptor–Bright test pattern and B/D indicates a Bright adaptor–Dark test pattern. Results in each column plot the log radial frequency amplitude ratio between the two test patterns at the PSE. In all the figures presented throughout this study, Error bars show the std. error of the mean for each observer, across trials.

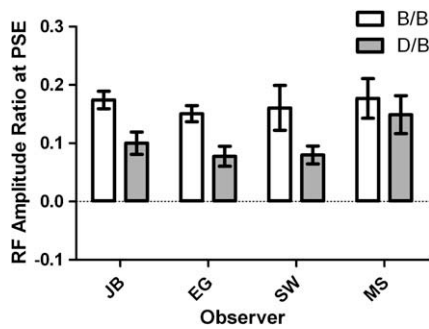


Fig. 3. RFAAEs for four observers when the angular phase of each adaptor and each test patterns was randomized on every trial, or every 500 ms for the adaptor. To conserve space, the observer is now shown on the x-axis and the adaptor-test combination is shown in the legend.

3.2. Experiment 2: local orientation?

To assess the contribution of local orientation adaptation to the RFAAE, consider first the size of the RFAAE in terms of the angular difference between RF contours at the PSE. The zero crossings of the test RF contours are the points where the orientation of the tangent to the curve differs maximally between different amplitudes. Thus it would make sense to compare the difference in tangent orientation at the PSE to the magnitude of the tilt after-effect (TAE) produced by adapting to line elements under similar conditions (see Section 2.3). It would also make sense to measure the luminance spatial-frequency selectivity of both the RFAAE and TAE. The TAE has been shown to be tightly tuned for this parameter (Roach et al., 2008; Ware & Mitchell, 1974), while sensitivity to RF shape is reportedly not (Wilkinson et al., 1998). If the RFAAE is just

the sum of local tilt after-effects, its magnitude should not only be consistent with that of the TAE but it should also be tightly tuned for luminance spatial-frequency.

Results are shown in Fig. 4. In all conditions, the test pattern had a luminance spatial-frequency of 8 cpd, while the spatial-frequency of the adaptor took on values of 8, 4 and 2 cpd, in separate conditions. Fig. 4A shows the size of both the TAE and RFAAE. For the TAE the adaptor and test patterns were in the same average spatial location, while for the RFAAE the adaptor and test patterns had the same mean radius and angular phase (RF contours). All patterns were independently spatially jittered on each trial (every 500 ms for the adapting patterns). The fig. reveals that both after-effects are large and significant when expressed as an angular distortion at the PSE ($F_{(3,12)} = 22.49, p < .0001$). The size of both after-effects decreases as the luminance spatial-frequency of the adapting stimuli was reduced relative to the test stimuli ($F_{(2,8)} = 13.63, p < .01$). Interestingly, the size of the angular distortion for the RFAAE and for the TAE was not significantly different ($F_{(1,8)} = 1.03, p = .36$). This indicates that the orientation shift in the TAE is not significantly different from that of the zero-crossing tangent in the RFAAE. This suggests that a local TAE can account for much of the RFAAE under these circumstances.

Previous reports have suggested that local adaptation strongly contributes to RF shape after-effects when the mean radius of the adapting and test patterns are the same, but importantly not when different (Anderson et al., 2007). This conclusion is consistent with research showing that the local TAE is tightly tuned for spatial location (Roach et al., 2008). To find out whether the RFAAE is more than a local TAE when adaptor and test patterns are not spatially coincident, we re-measured both after-effects under circumstances where the adaptors and test stimulated different retinal locations. For the RFAAE the adapting patterns had a mean radius of 1.5° and the test patterns 1°. For the TAE the adapting

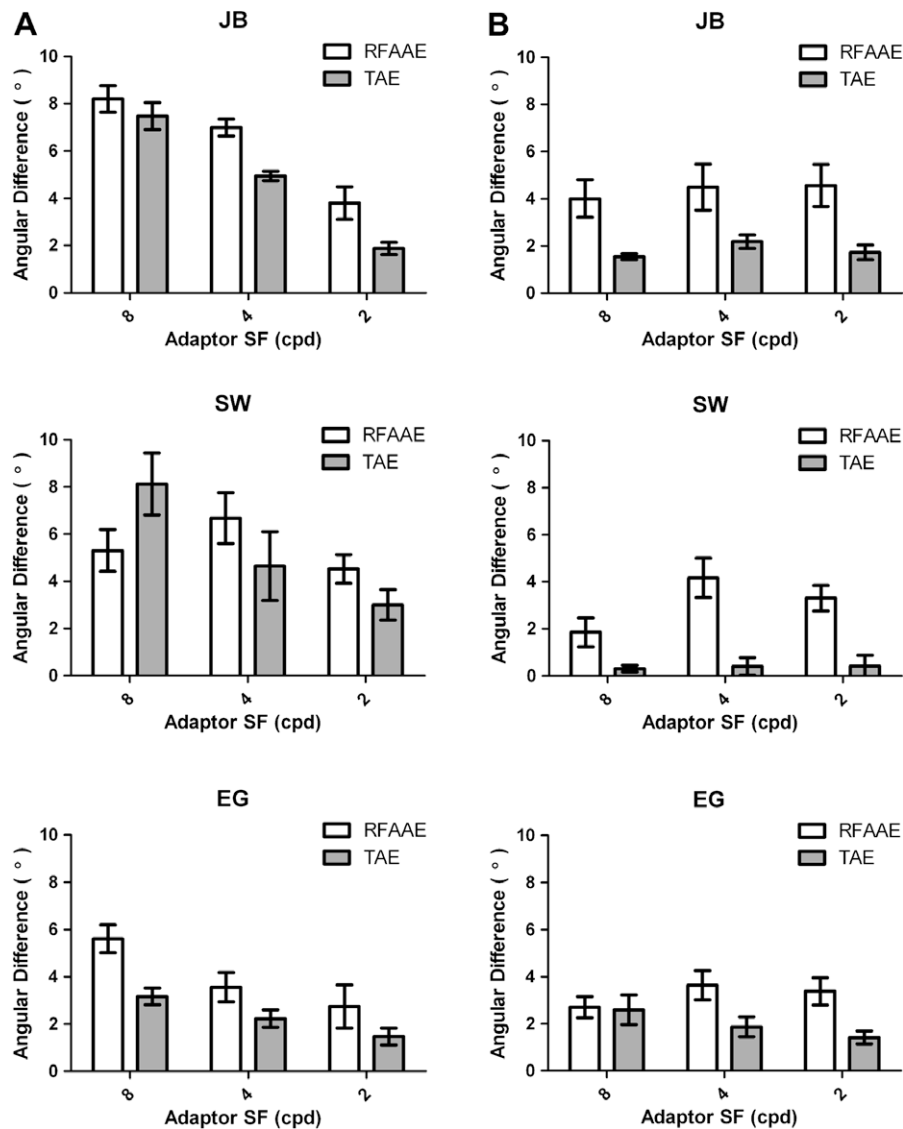


Fig. 4. RFAAEs (Clear bars) and TAEs (Grey bars) for three observers, when the adaptor and test were in the same spatial location 'A', or were in different spatial locations 'B'. Data columns show the average angular difference, in degrees (at the PSE following adaptation) between the upper and lower test patterns at the zero crossing (RFAAE) or between the orientation of the upper line element relative to the lower (TAE). The Horizontal axes describe the luminance spatial-frequency profile of the adapting patterns (the test was fixed at $8\text{ c}/^\circ$ in all conditions).

lines were offset 0.5° horizontally from the test lines. The length of the adapting line elements was scaled to be equal with the mean radius of the adapting RF pattern (although results for one observer, JB were the same irrespective of whether adaptor line length was scaled or not [data not shown]).

Fig. 4B shows RFAAEs and TAEs for the spatially offset adaptor/test conditions. A clear difference can now be seen between the two types of after-effect. RFAAEs are significantly different from baseline (repeated measures one-way ANOVA $F_{(3,11)} = 13.54$, $p < .01$) and are now significantly larger than TAEs ($F_{(1,8)} = 11.58$, $p < .01$). TAEs are not significantly different from baseline (ANOVA $F_{(3,11)} = 2.65$, $p > .05$). For observer EG, the difference between RFAAEs and TAEs is reduced compared with the other two observers but the difference between RFAAEs and TAEs is statistically significant ($F_{(1,9)} = 5.77$, $p < .05$).

The results of Experiment 2 show that when the adapting pattern and test pattern are in different retinal locations (i.e. of different average radii), RFAAEs cannot be explained by local TAEs alone. However, since local TAEs do appear to contribute to the RFAAE

when the adaptor and test have the same radii, it is sensible to re-measure selectivity for contrast polarity using different radii adaptor and test patterns (Experiment 3).

One further point of interest in Fig. 4B is that there is no significant decrease in the size of the RFAAE when the luminance spatial-frequency of the adapting RF patterns is varied relative to the test ($F_{(2,8)} = 5.42$, $p > .05$). This suggests that under these circumstances the RFAAE is not tuned for luminance spatial-frequency, even when measured across a fourfold range. This differs from the shape-frequency after-effect, which was reduced by approximately 50% when the adaptor and test differed in spatial-frequency by as little as a factor of two (Gheorghiu & Kingdom, 2006).

It has been suggested that the luminance spatial-frequency selectivity of after-effects such as the TAE is dependent upon the use of adaptor and test stimuli that are matched in relative contrast (i.e. multiples of contrast threshold), rather than physical contrast (Ware & Mitchell, 1974). It should be noted however that this has not been found in all TAE studies (Roach et al., 2008), the pres-

ent study included (see Fig. 4B). In our study, line and RF stimuli were matched for physical contrast only ($C = 0.99\%$ for all). The exact choice of physical or relative contrast matching is unlikely to influence shape after-effects for RF patterns because discrimination thresholds for RF patterns are agnostic to changes in a pattern's luminance contrast (Wilkinson et al., 1998); in other words RF-shape processing mechanisms do not appear to code this attribute.

To further investigate whether radial frequency shape after-effects are tuned to different parameters than those for sinusoidal contour shape after-effects, we measured the RFAAE tuning to parameters for which sine-wave shape after-effects are strongly tuned. One is luminance contrast polarity, the other pattern amplitude. Tuning to these parameters is tested in Experiments 3 and 4. To minimize the likelihood that local orientation adaptation could be influencing our results, the mean radii of the RF adapting patterns in these experiments is set to be greater than that of the RF test patterns by a factor of 1.5.

3.3. Experiment 3: contrast polarity tuning?

Experiment 1 produced mixed results as to whether the RFAAE is selective for luminance contrast polarity. We found large (~80%) transfer between opposite polarity adaptors and tests when both were fixed in angular phase but spatially jittered (Fig. 2), and moderate transfer (~60%) when both patterns were spatially fixed but randomly jittered in angular phase (Fig. 3). Given the results from Experiment 2 suggesting that when the adaptors and tests had different mean radii any after-effect was unlikely to be a manifestation of the tilt after-effect (Fig. 4B and see Anderson et al., 2007), it would seem prudent to re-measure selectivity for contrast polarity using this configuration.

Fig. 5 shows RFAAEs for three observers for a Bright test pair following adaptation to either a Bright (B/B = same), or Dark adapting pair (D/B = opposite). There is clearly either very little (EG) or no (JB and SW) selectivity for contrast polarity. A paired samples *t*-test (two-tailed) revealed no significant difference between the size of the RFAAE in the same (B/B) and opposite (D/B) polarity conditions ($t_{(2)} = 0.37, p = .74$). This is consistent with the data from Experiment 1 (Fig. 2) using adaptation and test pairs with the same angular phase and mean radius. It would appear however that although the TAE may have contributed significantly to the magnitude of the RFAAE in Experiment 1, this was not the reason for the weak selectivity to luminance contrast polarity.

Why is there only moderate (60%) transfer across contrast polarity for the random-phase adaptor and test pairs (Fig. 3)? It is possible that because the after-effect is smaller for the random-phase compared to fixed-phase RF pattern, the selectivity to

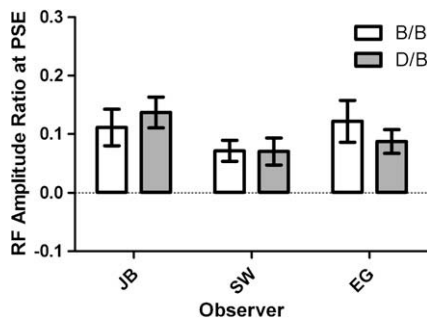


Fig. 5. RFAAEs for three observers following adaptation to RF contours which were either the same (B/B) or opposite (D/B) contrast polarity in relation to the Bright test pairs. In the data shown, the mean radii of the adapting RF pairs was 1.5° while the mean radii of the test RF pairs was 1°.

contrast polarity is not obscured by a ceiling effect. Alternatively, the random-phase RF patterns might be adapting local curvature rather than global shape, since local curvature has been shown to be contrast polarity selective (Gheorghiu & Kingdom, 2006). This possibility will be further explored in Experiment 5.

3.4. Experiment 4: amplitude tuning?

The shape amplitude after-effect (SAAE) is bi-directional, meaning that adaptation to a given amplitude results in a lower amplitude test appearing lower in amplitude and a higher amplitude test appearing higher in amplitude (Gheorghiu & Kingdom, 2007b). Is the RFAAE also bi-directional? We used the single adaptor method used previously by Gheorghiu and Kingdom (2007b) and described here in the General Methods (Section 2.3). The amplitude of the RF test pattern was fixed at $A = 0.1$, while the amplitude of the adapting RF pattern was systematically varied in log2 steps above and below this value, including a condition where the adaptor had zero amplitude ($A = 0$ in Eq. (1); a circle).

Fig. 6 shows the results for two observers. Black squares show the after-effect when adaptor and test had the same mean radius (1°), and grey squares when they had a different mean radius (adaptor 1.5°, test 1°). There is clear bi-directional tuning of the RFAAE. Interestingly, even adapting to a circle ($A = 0$) causes an increase in the perceived amplitude of an $A > 0$ test pattern. This result is somewhat surprising since the presence of a circle has no effect on the detection of an RF pattern with a different mean radius (Bell & Badcock, 2008; Habak, Wilkinson, & Wilson, 2006; Habak, Wilkinson, Zakher, & Wilson, 2004). The significance of this result will be discussed later.

Since the RFAAE exhibits similar bi-directional tuning to the SAAE (Gheorghiu & Kingdom, 2007b), it renews the possibility that

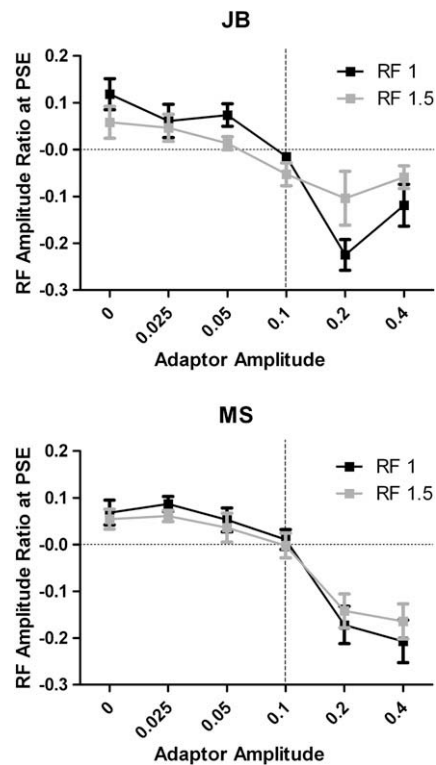


Fig. 6. Results for two observers showing the size and direction of the RFAAE as a function of the amplitude of the adapting RF contour (single adaptor method). Black square data points show results when the adaptor and test were the same mean radii (1°). Grey square data points show results when the mean radius of the adaptor was 1.5° and the mean radii of the test pairs was 1°.

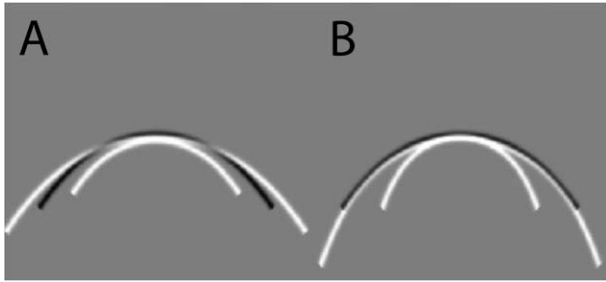


Fig. 7. Illustrates local RF pattern curvature across a single positive half cycle of radius modulation, from zero crossing to zero crossing (Amplitude = 0.1 [A] or 0.2 [B]). The black contour line in each figure shows the local curvature across one half cycle of the RF test pattern (fixed in all conditions at $A = 0.1$ and mean radius = 1.4°). White contour lines show a half cycle of modulation for the smallest 1° and largest 1.8° radii adapting patterns used in this experiment. For illustration purposes, the white contours have been nudged vertically, in order to allow a straight forward comparison of adaptor and test curvature at different radii and at different amplitudes however, this vertical shift does not in any way distort the curvature.

curvature adaptation rather than global-shape adaptation could underpin the RFAAE, even though the results of Experiments 2 and 3 do not support this conclusion. Therefore, Experiment 5 directly tests whether the RFAAE is consistent with local-curvature or global-shape adaptation.

3.5. Experiment 5: curvature adaptation or global-shape adaptation?

We employed a manipulation that allowed us to alter local curvature without altering global shape: radius change. This is illustrated in Fig. 7A and B). In both sides of Fig. 7, an example half-cycle curve of a test pattern with 1.4° radius is shown in black, and two half-cycle curves of adapting patterns with the largest differences in radii, 1° and 1.8° , shown in white. In the left Fig. 7A all three patterns have the same amplitude ($A = 0.1$) yet curvature decreases with increasing radius. In the figure on the right Fig. 7B, the same three radii patterns are shown, but now the adapting patterns (white) both have a higher amplitude ($A = 0.2$) than the test

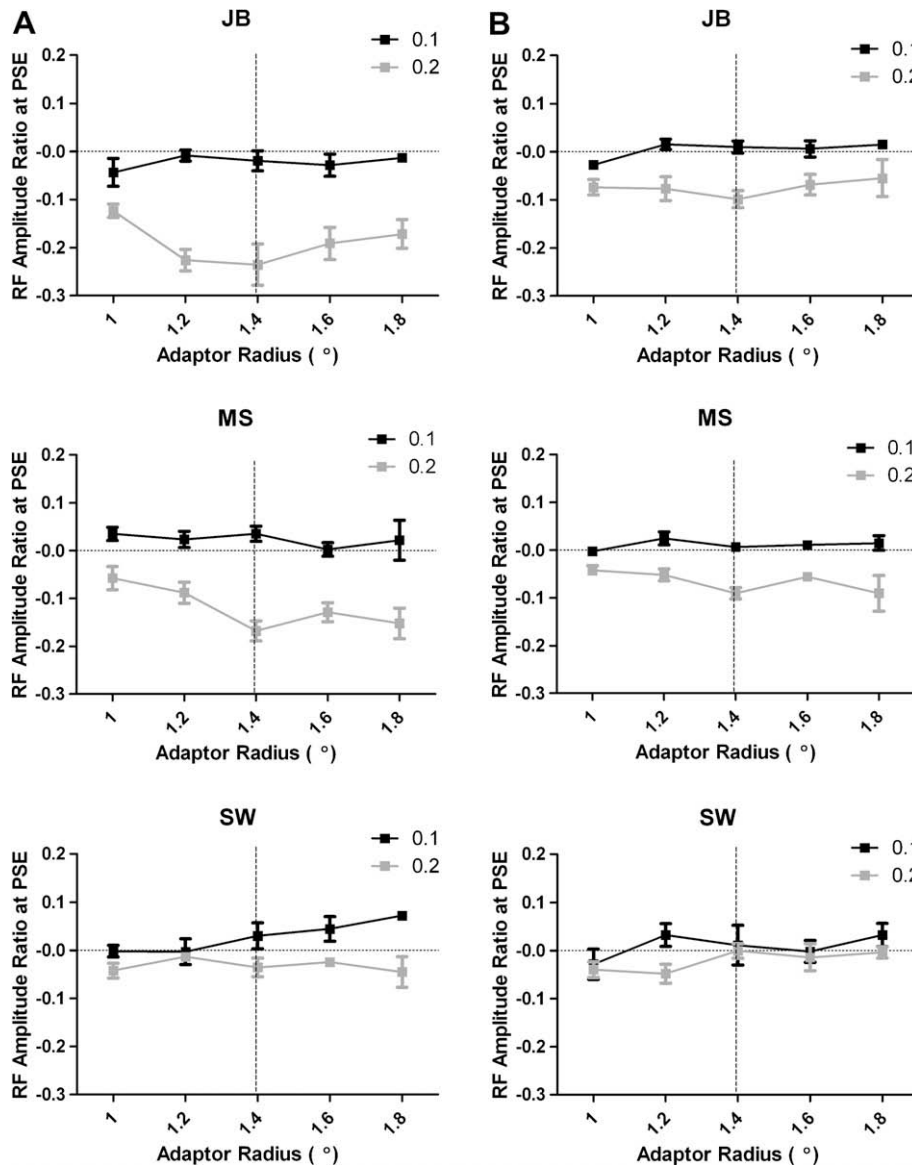


Fig. 8. RFAAEs for three observers as a function of adapting pattern radius and amplitude. Black square data points show results when the adaptor and test were the same amplitude ($A = 0.1$). Grey square data points show results when the amplitude of the adaptors was higher ($A = 0.2$) than that of the test pairs ($A = 0.1$). The horizontal axes indicate the mean radius of the adapting patterns. 'A' shows results when the adaptor and test pairs were fixed in relative angular phase but independently jittered in spatial position; 'B' shows results when the adaptor and test pairs were fixed in relative spatial location but individually randomly varied in angular phase.

(black) pattern ($A = 0.1$). In this case increasing the radius of the adapting pattern (white) makes its curvature more similar to the test pattern (black), culminating in the large radius adaptor being almost identical in curvature to that of the test.

If the RFAAE is driven by the global shape of the adaptor, then the after-effect should not be tuned for radius since changing the radius does not change global shape. On the other hand, if the RFAAE is tuned for local curvature then the after-effect would be expected to show strong tuning for radius since changing radius does change local curvature. We tested between the two possibilities using the single adaptor method (see Section 2.3), with the test pattern fixed in amplitude to 0.1.

Fig. 8A shows the results for three observers when the adaptors and tests were fixed in angular phase but independently spatially jittered on each trial (every 500 ms for the adapting pattern). Black squares show the after-effect when adaptor and test were in the corresponding location and equal in amplitude ($A = 0.1$). Grey squares show the after-effect when the adaptor had an amplitude of 0.2 and the test 0.1. Although observer SW shows weak radius tuning when the adaptor amplitude was 0.1, across observers and adaptor amplitudes the RFAAE shows no significant tuning for adaptor radius ($F_{(4,16)} = 0.47$, $p = .75$). The difference between the two amplitude conditions fell just short of significance ($F_{(1,16)} = 6.84$, $p = .059$), likely due to the small effect for observer SW. There was no interaction between adaptor amplitude and adaptor radius ($F_{(4,16)} = 1.87$, $p = .16$). These results show that the RFAAE is tuned for global shape not local curvature.

Fig. 8B shows results when the angular phase of the adapting and test pairs were independently randomized on each trial (every 500 ms for the adapting pattern) but fixed in relative spatial location. The results are similar to the fixed phase data, i.e. there is no effect of pattern radius ($F_{(4,16)} = 0.87$, $p = .5$) and no interaction between adaptor radius and adaptor amplitude ($F_{(4,16)} = 1.30$, $p = .31$). Although the after-effect is on average smaller than that for the fixed-phase conditions (Fig. 8A) there is a significant difference between adaptor amplitudes ($A = 0.2$ versus $A = 0.1$): $F_{(1,16)} = 11.79$, $p < .05$). While observer SW shows some signs of weak, but nonsystematic tuning for pattern radius; there is no indication of any tuning for radius in the data for the other two observers. Thus the random-phase data also appear to show that the RFAAE is tuned for global shape not local curvature.

4. General discussion

This study adds important new information to the shape-processing literature. We have revealed the existence of a novel, bidirectional global-shape after-effect in radial frequency (RF) patterns. The after-effect cannot be explained by local orientation adaptation alone (Fig. 4) or by local curvature adaptation alone (Fig. 8), and at least under some circumstances is not selective for luminance spatial-frequency (Fig. 4B), luminance polarity (Fig. 5) or pattern radius (Fig. 8). This suggests that these three attributes are not represented at the stage in vision where the global shape of RF patterns is encoded.

Despite evidence showing that RF patterns are represented by their points of curvature (Bell et al., 2008; Loffler et al., 2003; Poirier & Wilson, 2007), the finding that RF shape after-effects are agnostic to changes in low-level attributes such as luminance polarity and spatial-frequency, while curvature after-effects are not (Gheorghiu & Kingdom, 2006), has implications for current models of shape processing. It has been suggested that there is a common neurological site for processing both curvature fragments and global shape, with area V4 the likely candidate (Connor, 2004; Habak et al., 2004; Pasupathy & Connor, 1999, 2001, 2002; Poirier & Wilson, 2006). Our results however are not consistent with cur-

vature and global shape being processed by a common neural mechanism. An alternative explanation, which is consistent with recent literature, is that in addition to activating intermediate-level curvature processing mechanisms, RF patterns activate higher, object-related areas such as the Lateral Occipital Cortex (LOC) (Betts et al., 2008; Rainville, Yourganov, & Wilson, 2005). The involvement of an additional tier of processing could explain why RF-shape after-effects are agnostic to many low-level attributes while curvature-based after-effects are not.

The second aim of the study was to investigate whether differences in methodology underlay the differences in findings from recent curvature and RF-shape processing studies. It had been argued that in the context of contour-shape processing, appearance-based and performance-based tasks might tap quite different underlying processes (Gheorghiu & Kingdom, 2008; Loffler, 2008). To test this possibility it was necessary to use a common methodology, and after-effects of shape-amplitude were chosen to do this. We were able to demonstrate that RF patterns are represented differently from the components of the pattern, whether the components were orientations (Experiment 2) or curvatures (Experiment 5), and that RF patterns are not selective for luminance spatial-frequency or luminance contrast polarity. These findings are in keeping with previous performance-based studies (Bell & Badcock, 2008; Wilkinson et al., 1998).

With regard to how local curvature is encoded for global shape representation, Bell et al. (2008) have shown that both the angle and angular breadth of each curve in relation to the object center is important, in keeping with other detection studies showing that global shape representation is size invariant over a large range of radii (Achtman et al., 2000; Bell et al., 2008; Wilkinson et al., 1998). What has not been revealed in previous studies is that pattern amplitude/deformation is also a critical dimension for representing RF shapes, as our results show. Increasing pattern amplitude/deformation sharpens the degree of curvature represented at each local point on the contour. By showing that the RFAAE is a bi-directional after-effect (Fig. 6) we have revealed that the index of this local curvature is also an important parameter in global shape representation. This parameter is not accommodated in current RF pattern perception models (Poirier & Wilson, 2006). The results of recent contour curvature studies suggest that a population of curvature tuned neurons exist, which are individually selective for the 'sag' of a curve (Gheorghiu & Kingdom, 2007b, 2008; Hancock & Peirce, 2008; Pasupathy & Connor, 1999, 2001), implying that the neural hardware exists for representing different amplitudes of global shapes.

Also relevant for current models of RF-shape processing is our finding that adapting to a circle influences the perceived amplitude of an RF test (Fig. 6). In the recent literature on RF patterns, circles have been regarded as a distinct class of shape, processed by different mechanisms from RF patterns (Betts et al., 2008; Habak et al., 2004; Poirier & Wilson, 2006). Our findings suggest that instead a circle should be regarded as part of a continuum of RF patterns.

Previous studies on RF pattern adaptation (Anderson et al., 2007; Bell et al., 2008), masking (Bell & Badcock, 2008, 2009; Habak et al., 2004, 2006) and detection (Bell, Badcock, Wilson, & Wilkinson, 2007b; Jeffrey et al., 2002; Loffler et al., 2003; Wilkinson et al., 1998) have employed global shapes centered on the observer's fixation. The shapes in our study were all positioned eccentrically. The compatibility of most of our results with these previous studies indicates that global-shape mechanisms are insensitive to small variations in the position of the shape relative to the observer's fixation. In addition, an extrapolation of the data at the appropriate points on the amplitude tuning function (single adaptor method) in Fig. 6 (0.05 or 0.15) indicates that neither adaptor in isolation would have been able to produce the size of RFAAEs re-

ported in the analogous dual adaptor experiments (e.g. Figs. 2 and 8), suggesting that both RF adaptors were processed in parallel.

5. Conclusions

We have introduced a novel shape-amplitude after-effect involving radial frequency patterns, the RFAAE, an analog of the shape-amplitude after-effect involving sinusoidal-shaped contours (Gheorghiu & Kingdom, 2007b). We have shown that the RFAAE is almost certainly mediated by global-shape adaptation, rather than local orientation or curvature adaptation. In turn we have revealed that the representation of a global shape is qualitatively different from the representation of the parts that make up the shape. The differences we found between fixed and randomly-oriented RF shapes imply that global-shape mechanisms are not rotation invariant but tuned for absolute orientation, as suggested by others (Bell et al., 2008; Hess, Achtman, & Wang, 2001). Finally we have shown that RF pattern processing is tuned for shape amplitude. The current model of RF pattern perception (e.g. Poirier and Wilson, 2006) needs to be revised in light of these findings.

References

- Achtman, R. L., Hess, R. F., & Wang, Y. Z. (2000). Regional sensitivity for shape discrimination. *Spatial Vision*, 13(4), 377–391.
- Anderson, N. D., Habak, C., Wilkinson, F., & Wilson, H. R. (2007). Evaluating shape after-effects with radial frequency patterns. *Vision Research*, 47(3), 298–308.
- Attneave, F. (1954). Some informational aspects of visual perception. *Psychological Review*, 61(3), 183–193.
- Badcock, D. R., & Clifford, C. W. (2006). The inputs to global form. In M. Jenkins & R. Harris (Eds.), *Seeing spatial form* (pp. 37–50). Oxford: Oxford University Press.
- Bell, J., & Badcock, D. R. (2009). Narrow-band radial frequency shape channels revealed by sub-threshold summation. *Vision Research*, 49(8), 843–850.
- Bell, J., & Badcock, D. R. (2008). Luminance and contrast cues are integrated in global shape detection with contours. *Vision Research*, 48(21), 2336–2344.
- Bell, J., Badcock, D., Wilson, H., & Wilkinson, F. (2007a). Detection of global shape in radial frequency patterns involves interacting contour shape channels operating independently of local form processes. *Journal of Vision*, 7(9), 920.
- Bell, J., Badcock, D. R., Wilson, H., & Wilkinson, F. (2007b). Detection of shape in radial frequency contours: Independence of local and global form information. *Vision Research*, 47(11), 1518–1522.
- Bell, J., Dickinson, J. E., & Badcock, D. R. (2008). Radial frequency adaptation suggests polar-based coding of local shape cues. *Vision Research*, 48(21), 2293–2301.
- Betts, L., Rainville, S., & Wilson, H. (2008). Adaptation to radial frequency patterns in the lateral occipital cortex. *Journal of Vision*, 8(6), 723.
- Biederman, I. (1987). Recognition-by-components: A theory of human image understanding. *Psychological Review*, 94(2), 115–147.
- Burke, D., Taubert, J., & Higman, T. (2007). Are face representations viewpoint dependent? A stereo advantage for generalising across different views of faces. *Vision Research*, 47(16), 2164–2169.
- Connor, C. E. (2004). Shape dimensions and object primitives. In L. M. Chalupa & J. S. Werner (Eds.), *The visual neurosciences* (pp. 1080–1089). London: MIT Press.
- Gheorghiu, E., & Kingdom, F. A. (2006). Luminance-contrast properties of contour-shape processing revealed through the shape-frequency after-effect. *Vision Research*, 46(21), 3603–3615.
- Gheorghiu, E., & Kingdom, F. A. (2007a). Chromatic tuning of contour-shape mechanisms revealed through the shape-frequency and shape-amplitude after-effects. *Vision Research*, 47(14), 1935–1949.
- Gheorghiu, E., & Kingdom, F. A. (2007b). The spatial feature underlying the shape-frequency and shape-amplitude after-effects. *Vision Research*, 47(6), 834–844.
- Gheorghiu, E., & Kingdom, F. A. (2008). Spatial properties of curvature-encoding mechanisms revealed through the shape-frequency and shape-amplitude after-effects. *Vision Research*, 48(9), 1107–1124.
- Grill-Spector, K., Kushnir, T., Edelman, S., Avidan, G., Itzhak, Y., & Malach, R. (1999). Differential processing of objects under various viewing conditions in the human lateral occipital complex. *Neuron*, 24(1), 187–203.
- Grill-Spector, K., Kushnir, T., Edelman, S., Itzhak, Y., & Malach, R. (1998). Cue-invariant activation in object-related areas of the human occipital lobe. *Neuron*, 21(1), 191–202.
- Habak, C., Wilkinson, F., & Wilson, H. R. (2006). Dynamics of shape interaction in human vision. *Vision Research*, 46(26), 4305–4320.
- Habak, C., Wilkinson, F., Zakher, B., & Wilson, H. R. (2004). Curvature population coding for complex shapes in human vision. *Vision Research*, 44(24), 2815–2823.
- Hancock, S., & Peirce, J. W. (2008). Selective mechanisms for simple contours revealed by compound adaptation.
- Hess, R. F., Achtman, R. L., & Wang, Y. Z. (2001). Detection of contrast-defined shape. *Journal of the Optical Society of America A – Optics Image Science and Vision*, 18(9), 2220–2227.
- Hess, R. F., Wang, Y. Z., & Dakin, S. C. (1999). Are judgements of circularity local or global? *Vision Research*, 39(26), 4354–4360.
- Jeffery, L., Rhodes, G., & Busey, T. (2006). View-specific coding of face shape. *Psychological Science*, 17(6), 501–505.
- Jeffrey, B. G., Wang, Y. Z., & Birch, E. E. (2002). Circular contour frequency in shape discrimination. *Vision Research*, 42(25), 2773–2779.
- Lamme, V. A., Super, H., & Spekreijse, H. (1998). Feedforward, horizontal, and feedback processing in the visual cortex. *Current Opinion in Neurobiology*, 8(4), 529–535.
- Lennie, P. (1998). Single units and visual cortical organization. *Perception*, 27(8), 889–935.
- Lerner, Y., Hendler, T., Ben-Bashat, D., Harel, M., & Malach, R. (2001). A hierarchical axis of object processing stages in the human visual cortex. *Cerebral Cortex*, 11(4), 287–297.
- Loffler, G. (2008). Perception of contours and shapes: Low and intermediate stage mechanisms. *Vision Research*, 48(20), 2106–2127.
- Loffler, G., Wilson, H. R., & Wilkinson, F. (2003). Local and global contributions to shape discrimination. *Vision Research*, 43(5), 519–530.
- Loffler, G., Yourganov, G., Wilkinson, F., & Wilson, H. R. (2005). fMRI evidence for the neural representation of faces. *Nature Neuroscience*, 8(10), 1386–1390.
- Magnussen, S., & Kurtenbach, W. (1979). A test for contrast-polarity selectivity in the tilt after effect. *Perception*, 8(5), 523–528.
- Murray, S. O., & He, S. (2006). Contrast invariance in the human lateral occipital complex depends on attention. *Current Biology*, 16(6), 606–611.
- Murray, S. O., Kersten, D., Olshausen, B. A., Schrater, P., & Woods, D. L. (2002). Shape perception reduces activity in human primary visual cortex. *Proceedings of the National Academy of Sciences of the United States of America*, 99(23), 15164–15169.
- Okusa, T., Kakigi, R., & Osaka, N. (2000). Cortical activity related to cue-invariant shape perception in humans. *Neuroscience*, 98(4), 615–624.
- Pasupathy, A., & Connor, C. E. (1999). Responses to contour features in macaque area V4. *Journal of Neurophysiology*, 82(5), 2490–2502.
- Pasupathy, A., & Connor, C. E. (2001). Shape representation in area V4: Position specific tuning for boundary conformation. *Journal of Neurophysiology*, 86, 2505–2519.
- Pasupathy, A., & Connor, C. E. (2002). Population coding of shape in area V4. *Nature Neuroscience*, 5(12), 1332–1338.
- Poirier, F. J. A. M., & Wilson, H. R. (2006). A biologically plausible model of human radial frequency perception. *Vision Research*, 46(15), 2443–2455.
- Poirier, F. J., & Wilson, H. R. (2007). Object perception and masking: Contributions of sides and convexities. *Vision Research*, 47(23), 3001–3011.
- Rainville, S. P. J., Yourganov, G., & Wilson, H. R. (2005). Closed-contour shapes encoded through deviations from circularity in lateral-occipital complex (LOC): An fMRI study. *Journal of Vision*, 5(8), 471.
- Roach, N. W., Webb, B. S., & McGraw, P. V. (2008). Adaptation to global structure induces spatially remote distortions of perceived orientation. *Journal of Vision*, 8(3), 31, 1–12.
- Ware, C., & Mitchell, D. E. (1974). The spatial selectivity of the tilt aftereffect. *Vision Research*, 14(8), 735–737.
- Wilkinson, F., Wilson, H. R., & Habak, C. (1998). Detection and recognition of radial frequency patterns. *Vision Research*, 38(22), 3555–3568.
- Wilson, H. R., & Wilkinson, F. (1998). Detection of global structure in glass patterns: Implications for form vision. *Vision Research*, 38(19), 2933–2947.
- Wilson, H. R., Wilkinson, F., & Asaad, W. (1997). Concentric orientation summation in human form vision. *Vision Research*, 37(17), 2325–2330.